

Mapping and characterizing land deformation over the Gulf Coast using multi-temporal InSAR

Feifei Qu¹, Zhong Lu¹, Jinwoo Kim¹, Michael J. Turco²

¹ Roy M. Huffington Department of Earth Sciences, Southern Methodist University, Dallas, Texas, USA, 75025;

² Harris-Galveston Subsidence District, Friendswood, Texas, USA, 77546.

Contact: zhonglu@smu.edu

Abstract

Land subsidence has occurred in the Gulf Coast (GC) of the U.S. as a consequence of complex geological conditions and high-intensity resource exploitation, causing extensive damage to buildings and other infrastructures. Using 1650 images from 33 ALOS-1 paths during 2007-2011 based on multi-temporal interferometric synthetic aperture (InSAR) techniques, we have constructed, for the first time, a deformation map over 500,000 km² of the 1900-km-long GC, with an RMSE of <10 mm/yr. Numerous land deformation zones have been discovered, including at least 30 subsidence patterns and 14 uplift features. Most of the identified ground instabilities are newly discovered as a result of this study. The land deformation along GC is caused by both regional geological conditions and human activities that have influenced natural surroundings and consequentially exacerbated ground instability. Depressurization of petroleum reservoirs and aquifer compaction related to groundwater withdrawal are the principal impactors on observed subsidence. Other processes, including wastewater injection, sulfur/salt mining, dewatering, oxidation, and construction work, also contributed to the ground instability. Our large-scale deformation mapping will help the scientific community and relevant agencies better understand land deformation rates and extents, identify the processes responsible for the coastal deformation, and provide a critical dataset for hazard prediction and mitigation in the GC.

Introduction

Subsidence is a nationwide problem: ~44,000 km² in 45 states of the U.S. have been permanently subsided (Galloway 2008). The GC has been exposed to land deformation due to its complicated geological constitution and high intensity of land use. The goal of this study is to provide a complete map of land deformation rates and extents over 500,000 km² of the 1900-km-long GC and identify the processes responsible for the coastal deformation using InSAR imagery and auxiliary data source. By employing the multi-temporal InSAR (MTI) techniques (Hooper 2008) and L-band SAR images from ALOS-1 (2007-2011), this work provides, for the first time, a comprehensive analysis of spatial distribution and characteristics of land deformation at a finer spatial resolution over a large span of the GC. This paper summarizes the discovered instability zones and major deformation features (Qu et al. 2023).

Methods, datasets, and processing

About 1650 SAR images from 33 ascending L-band ALOS PALSAR tracks have been utilized in this study to illustrate the spatial distributions of land deformation over the whole GC. The overlap area of about 10 km between neighboring ALOS tracks was used for validating and mosaicking. Ionospheric anomalies were present in some interferograms where the split-spectrum method was applied to mitigate the phase error. The 33 data stacks were then processed using the StaMPS MTI method (both PS and SBAS, respectively) (Hooper 2008). A deramp processing was also applied to interferograms to eliminate the residual orbital error and long-wavelength atmospheric error. Finally, remaining tropospheric artifacts were further estimated and mitigated through temporal high-pass filtering and spatial low-pass filtering. Innocuous turbulent tropospheric delays might still reside in some interferograms due to the limited number of ALOS-1 images in each track. Please refer to Qu et al. (2023) for detailed processing procedures.

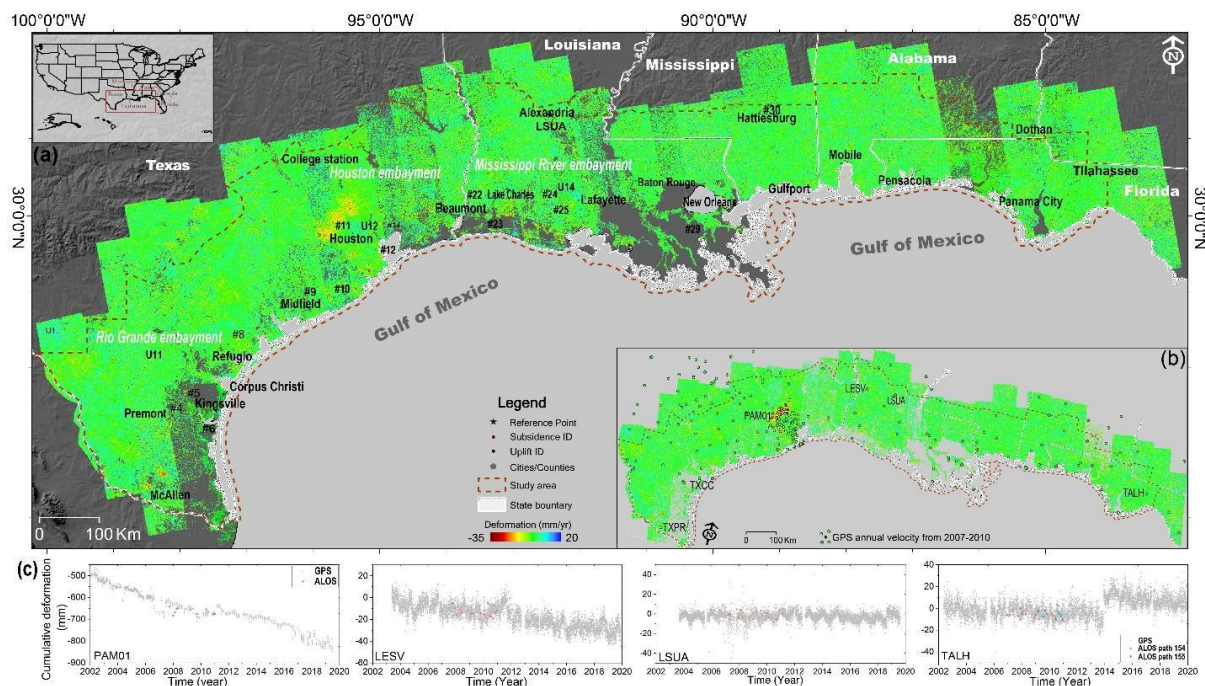


Figure 1 A seamless deformation map over 500,000 km² areas of GC: (a) Average vertical deformation map over GC by mosaicking InSAR products from 33 ALOS-1 tracks; (b) Comparison of the average vertical deformation rate between InSAR and GPS measurements during 2007-2011 at stations established after 2009 (Blewitt 2018); (c) Comparison between InSAR-derived time series deformation and GPS observations at 4 stations, whose locations were marked on (b); The “#1 - #30” label the measured subsidence zones and “U1-U14” indicate the identified uplift features. The U.S. map is an inset on the upper-left, where the red solid rectangle shows the approximate extent of (a).

A total of 33 average line-of-sight (LOS) deformation velocities between 2007 and 2011 were generated utilizing the MTI method. The deformations were transferred into the vertical direction according to the incidence angles to minimize the effects of imaging geometry. Overall, there is a generally good agreement for both the patterns and rates of deformation between adjacent tracks before mosaicking. To generate a seamless velocity map of GC all stacks were referenced to LASU Continuously Operating Reference Station (CORS) (black star, Fig.1a), situating at Rapides County, LA, where there was a wealth of high coherence points around and almost no deformation was observed at this station since Aug 31, 2003 (Blewitt et al. 2018). The average standard deviation of the 32 differential maps over the overlapped regions of neighboring tracks is ~ 9 mm/yr. Finally, a seamless deformation map over about 500,000km² areas of GC was produced for the first time by mosaicking 33 ALOS tracks (Fig.1).

Results

The GC is generally stable, but numerous land deformation zones have been realized, including at least 30 subsidence patterns and 14 uplift features (Fig.1). InSAR-derived average deformation observations were compared with velocity measurements from 190 GPS stations coastal-wide (Blewitt et al. 2018). Time-series deformation plots at 4 GPS stations, whose positions can be found in Fig.1b, are also shown in Fig.1c. There is a universal agreement between the daily/monthly GPS solutions and the InSAR time-series measurements (Fig.1c), with an average RMSE (root mean square error) of approximately 10 mm/yr for the difference between vertical deformation measurements from InSAR and GPS.

We observed broad-scale subsidence caused by groundwater pumping near major metropolitan areas, such as Houston and New Orleans (Fig. 1). We have found some of the published subsidence zones have ceased to be detectable from 2007 to 2011 while continuing deformation has been observed at the Greater Houston and New Orleans regions at reduced rates. Our InSAR-derived deformation map has also allowed us to discover one new subsidence feature caused by groundwater withdrawal at Beaumont, TX.

More than 20 subsidence cones with a velocity larger than 10 mm/yr have been detected through our MTI analysis over the GC, including particularly striking ground settlement patterns over Hidalgo County, TX, and Corpus Christi, TX (Fig. 2a). The subsidence patterns, with spatial scales ranging from 1 to 10 km in diameter, were likely caused by hydrocarbon extraction.

Subsidence of ~60 mm/yr has also been recognized at The Five Islands of Louisiana. The high spatial correlation between subsidence and salt mining systems as well as the absence of oil/gas exploration activities indicate that the conventional room-and-pillar salt mining method depending on heavy machinery in the underground could be responsible for the observed subsidence at Avery Island (Fig. 2b), Weeks Island, and Cote Blanche Island.

Our study revealed a high subsidence rate localized to construction-related areas on the south bank of the Mississippi River, mainly Jefferson Parish, providing insight into shallow sediment compaction as a causal factor of subsidence (Fig. 2c). The occurrence of shallow sediment compaction due to construction loading could last longer than a decade following the construction over the New Orleans area.

Finally, we identified significant uplift signals with amplitudes ranging from 3~10 cm/yr mainly over Duval County of South TX (Fig. 2d). At least 11 cones of uplift that are roughly circular and typically span ~2 km in diameter have been discovered, almost all of which had never been noticed and reported before this study. Our InSAR observations indicate a localized uplift feature occurs over the storage facilities, which fluctuates over time, responding to the seasonal nature of gas injection operations in summer. We attribute the recognized localized uplift signal over the North Dayton salt dome gas storage facility to the circulated operations of injection/withdrawal into/from the salt cavern.

Conclusion

This paper presents the land deformation of the GC during 2007-2011 and unveils the related geohazards by using satellite radar image processing techniques. We have constructed, for the first time, a deformation map for 500,000 km² over the Gulf Coast, spanning ~1900 km from east to west. The accuracy of the InSAR observations of deformation is 10 mm/yr based on comparison with GPS measurements. Ground deformation over the GC is not solely attributed to a single cause, but a combination of several different factors that involve large volumes of extraction of underground reservoirs (water, hydrocarbons, sulfur, and salt) and wastewater injection, as well as processes of sediment compaction, tectonics, and gravity-driven process. Our results enhance the understanding of the state of land deformation and causal mechanisms in the GC and are critically important for hazard prediction and mitigation in the region.

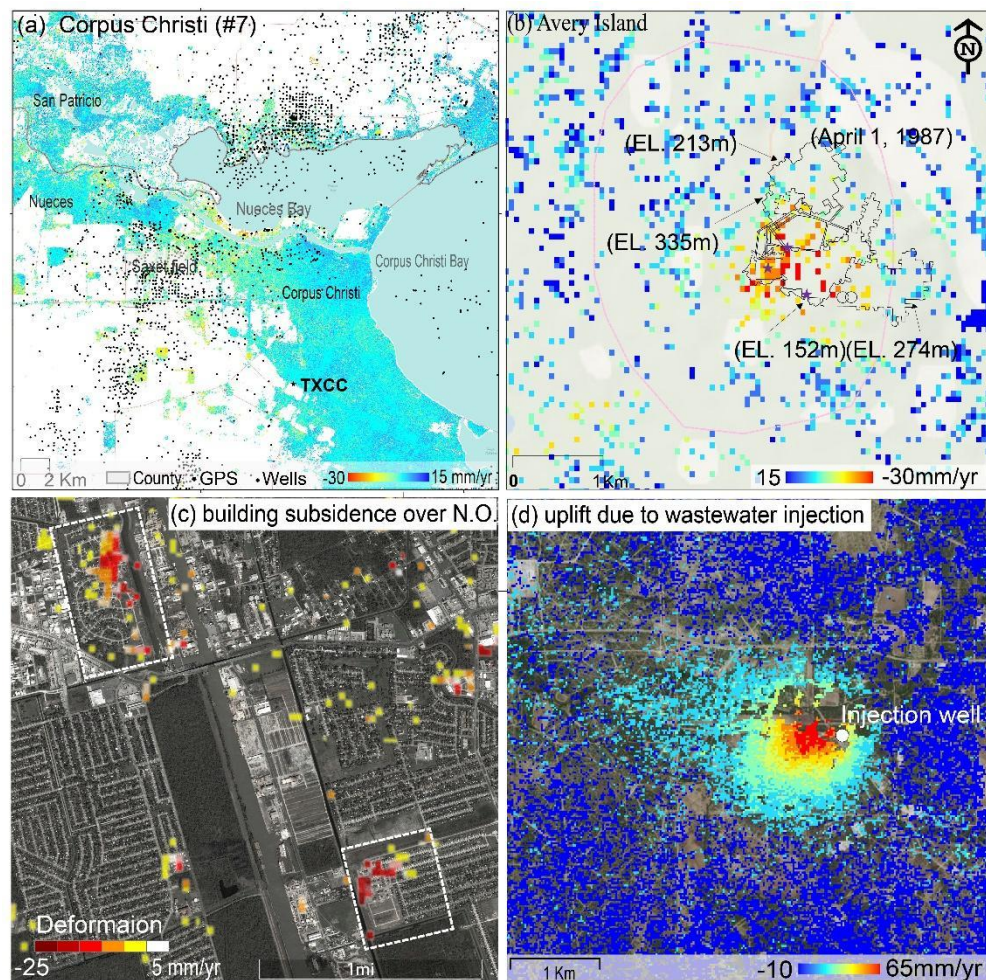


Figure 2 Highlights of deformation features observed along the GC. (a) Land subsidence caused by hydrocarbon extraction at Corpus Christi, Texas. (b) Ground subsidence due to underground mining at Avery Island, Louisiana. (c) Building subsidence due to sediment compaction at Jefferson Parish, Louisiana. (d) Ground uplift due to wastewater disposal over Duval County, Texas.

References

Blewitt, G., Hammond, W.C., Kreemer, C. (2018). Harnessing the GPS Data Explosion for Interdisciplinary Science. *Earth & Space Science News*, 99.

Hooper, A. (2008). A multi-temporal InSAR method incorporating both persistent scatterer and small baseline approaches. *Geophysical Research Letters*, 35, L16302.

Qu, F., Lu, Z., Kim, J.W., Turco, M.J. (2023). Mapping and characterizing land deformation during 2007-2011 over the Gulf Coast by L-band InSAR: *Remote Sensing of Environment*, 284, 113342, <https://doi.org/10.1016/j.rse.2022.113342>.